Analytical and Bioanalytical Chemistry (2022) 414:2513–2522
https://doi.org/10.1007/s00216-022-03892-0

RESEARCH PAPER

Development of a high-pH reversed-phase well plate for peptide fractionation and deep proteome analysis of cells and exosomes

Yu-Ching Liu[1,2] · Yu-Ting Huang[3] · Chao-Jung Chen[1,2]

Received: 10 November 2021 / Revised: 27 December 2021 / Accepted: 10 January 2022 / Published online: 31 January 2022
© Springer-Verlag GmbH Germany, part of Springer Nature 2022

Abstract

The complexity of the proteome often limits the number of identified proteins in the nanoflow LC-MS (nanoLC-MS) analysis of samples. Therefore, peptide fractionation is essential for reducing the sample complexity and improving the proteome coverage. In this study, to achieve high-pH reversed-phase (RP)-well plate fractionation for high-throughput proteomics analysis, C18 particles were coated on a 96-well plate, and the sample-loading processes were optimized for high-pH fractionation. The sample capacity of the high-pH RP-well plate was estimated to be ~6 μg of protein. There were 1.85- and 1.71-fold increases in the number of protein groups and peptides identified, respectively, with high-pH RP-well plate fractionation, compared to those without fractionation. In addition, with alkaline C18 well plate fractionation, exosome markers could be detected using ~1 μg of a protein digest of exosomes by microflow LC-MS (microLC-MS). These results illustrate that high-pH RP-well plate fractionation has superior sensitivity and effectiveness in preparing trace amounts of proteins for deep proteome analysis.

Keywords High-pH reversed-phase · Peptide fractionation · Proteomics · 96-well plate · Exosomes

Abbreviations

FA	Formic acid
FBS	Fetal bovine serum
FDR	False discovery rate
SEC	Size-exclusion chromatography

Introduction

Bottom-up proteomic approaches using proteolytic digestion result in biological samples that contain hundreds of thousands of peptides that span a wide range of concentrations [1]. Nano/microflow liquid chromatography–mass spectrometry (LC-MS) has become a powerful tool for identification and quantification in deep proteomics analysis. The increased sensitivity of MS techniques has allowed for the analysis of trace and valuable samples. However, the use of one-dimensional nano/microflow LC-MS is usually insufficient to resolve complex biological mixtures, limiting the number of identified proteins. Therefore, prior to MS analysis, fractionation methods are usually applied to reduce the complexity of the digested peptides for improving the sensitivity and specificity of protein identification.

Low-pH reversed-phase (RP) nano/microflow LC-MS with acid mobile-phase elution for peptide separation is the most commonly used dimension for direct coupling to nano-electrospray ionization–mass spectrometry (ESI-MS). To further reduce the sample complexity, various strategies for peptide separation prior to low-pH RP LC-MS analysis have been developed, including strong cation exchange (SCX) [2–4], OFFGEL electrophoresis [5, 6], hydrophilic interaction chromatography (HILIC) [7], size-exclusion chromatography (SEC) [8], and high-pH RP-LC [9, 10]. Because the pH change between high-pH RP and low-pH RP has a dramatic effect on peptide charge distribution, resulting in a different hydrophobicity in each dimension [11], high-pH RP has been shown to be semi-orthogonal to low-pH RP. Using a volatile-salt buffer in high-pH RP-LC to elute peptides can reduce the sample preparation time and decrease sample losses, rendering the method more suitable for handling trace samples prior to nano-LC-MS/MS. [10, 12]

✉ Chao-Jung Chen
cjchen@mail.cmu.edu.tw

1 Graduate Institute of Integrated Medicine, China Medical University, Taichung, Taiwan

2 Proteomics Core Laboratory, Department of Medical Research, China Medical University Hospital, Taichung, Taiwan

3 Exonox Biosciences, Inc., Taipei, Taiwan

LC column [10], HLB cartridge [13], and tip-based methods [14] have been reported for high-pH RP fractionation. However, LC column and HLB cartridge fractionation strategies often use large sample amounts and may result in significant sample loss for trace sample amounts. Tip-based methods are usually adopted for low protein amounts (< 10 µg) [15]; however, their loading volume is limited by the tip size, necessitating repetitive pipetting steps for larger sample volumes [16]. Furthermore, tips may sometimes be blocked by contaminating particles or proteins aggregated in high concentrations of organic solvents, resulting in increased back pressure, and making manual operation difficult or even unfeasible. Previously, we developed a rapid and simple approach for coating C18-functionalized plates by bonding silica-based functionalized particles on a polydimethylsiloxane (PDMS) membrane, called a CP plate. [17] A CP plate is a C18-functionalized plate suitable for peptide and protein purification. However, a flat C18 plate system cannot be directly applied to solvents with high hydrophilic properties (> 60% H_2O), because the strong repulsion force between the hydrophilic sample solution and the hydrophobic C18 surface results in a greater contact angle between sample solution droplet and a C18 spot. Hence the sample droplet is not easily located on a C18 surface. Therefore, on a flat C18 plate system, it is hard to observe the sample deposition area for the subsequent washing and fractionation steps, making the system unsuitable for peptide fractionation.

In this study, we present a newly designed C18-coated well plate that overcomes the aforementioned limitation by applying a larger sample volume to a sample well coated with C18 at the bottom of the well. Using this plate, a hydrophilic solvent can be used for peptide fractionation. The RP-well plate operation processes were optimized and used for high-pH peptide fractionation. The performance of the RP-well plate was demonstrated using a hepatoma cell line (HepG2) and exosome proteins from ovarian cancer cells (SKOV3) for deep proteome profiling.

Materials and methods

Chemicals and reagents

The polydimethylsiloxane (PDMS) prepolymer was purchased from Dow Corning (Sylgard® 184, Midland, MI, USA). Acetonitrile (ACN), formic acid (FA), and NH_4OH were purchased from J.T.Baker (Phillipsburg, NJ, USA). Ammonium formate, dithiothreitol (DTT), and iodoacetamide (IAA) were purchased from Sigma-Aldrich (St. Louis, MO, USA). Trypsin (modified, sequencing grade) was obtained from Promega (Madison, WI, USA). The HepG2 liver hepatocellular cell line and SKOV3 ovarian cancer cell line (Bioresource Collection and Research Center, Hsinchu, Taiwan) were kindly provided by Dr. Ping-Hsiao Shih (Department of Medical Research, China Medical University Hospital, Taiwan).

Fabrication of C18-coated RP-well plate

A flowchart of the C18-particle-coated RP-well plate fabrication and peptide fractionation is shown in Fig. 1. The

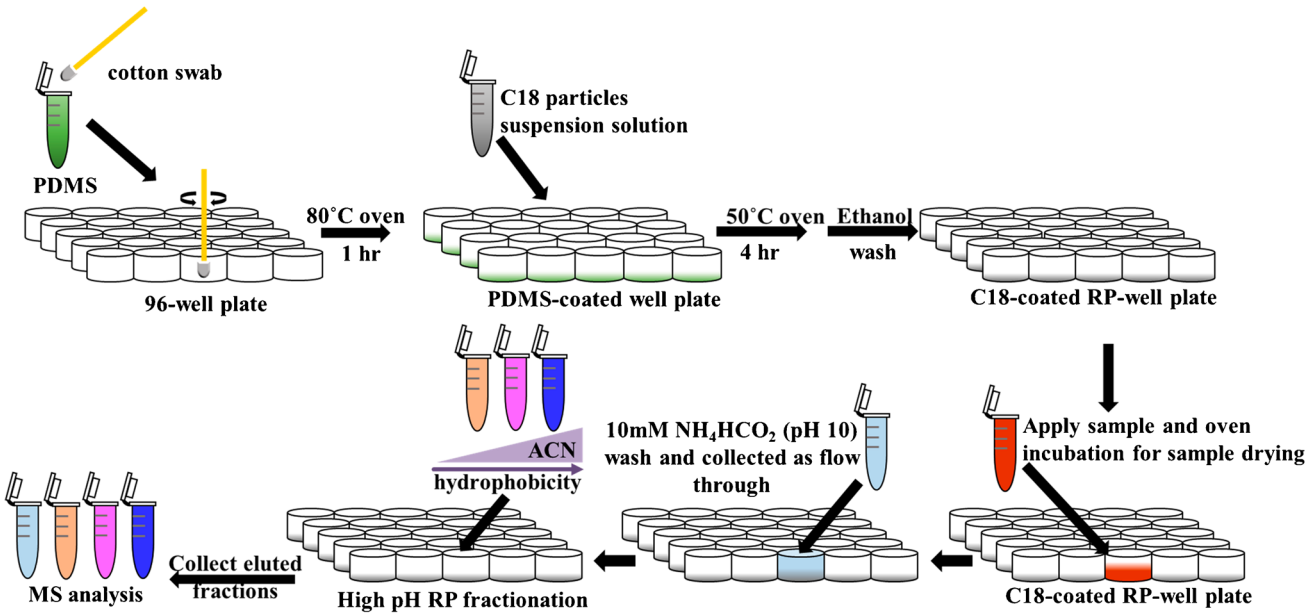

Fig. 1 Schematic representation of the functionalized RP-well plate fabrication and peptide fractionation procedures

PDMS prepolymer (reagent A) was mixed in a 1.5 mL tube with its curing agent (reagent B) in a 10:1 volume ratio and spun down. A cotton swab was dipped into the PDMS solution and then smeared on the bottom of sample wells of a 96-well plate to form a thin layer on the bottom of the well plate, which was then incubated in an oven for polymerization at 80 °C for 1 h. After the PDMS film formed, 60 µL of the C18 particle solution (1.7 µm, 130 Å, BEH, Waters; 3 mg in 1 mL, 80% ACN) was loaded on the PDMS-coated well plate; the plate was then incubated in an oven at 50 °C for 4 h. The excess C18 particles were flushed out with ethanol. The C18-coated RP-well plate was air-dried at room temperature and was then ready for use.

MALDI-TOF-MS analysis

Peptides were analyzed by MALDI-TOF/TOF-MS (Ultraflex III TOF/TOF; Bruker Daltonics) equipped with a Smartbeam laser. Peptide mass calibration for MALDI-TOF was performed with a peptide calibration standard kit (Bruker Daltonics) for a mass range of 800–4000 Da. The spectra were acquired in the reflectron mode using an accelerating voltage of 25 kV and a reflectron voltage of 26.3 kV. The mass spectra were processed using FlexAnalysis software (Bruker Daltonics).

Cell culture and lysis of HepG2 cell line

The human hepatocellular carcinoma cell line, HepG2, was grown in a DMEM medium supplemented with 10% fetal bovine serum (FBS, Thermo Fisher Scientific, USA) and 1% penicillin/streptomycin (P/S), and was maintained at 37 °C in a 5% CO_2 atmosphere. Cell pellets were harvested by washing cultures with cold PBS and lysing in RIPA lysis buffer (50 mM Tris-HCl, pH 7.5, 50 mM NaCl, 1% Nonidet P-40, 1% sodium deoxycholate, 0.1% SDS, 2 mM EDTA, and protease inhibitor). The cell lysate was centrifuged at 12,000 rpm for 20 min at 4 °C, and the supernatant was discarded.

SKOV3 exosome isolation and protein extraction

The highly invasive ovarian cell line, SKOV3, was grown in McCoy's 5A medium supplemented with 10% FBS and 1% P/S, and maintained at 37 °C in a 5% CO_2 atmosphere. Once the SKOV3 cells grew to greater than 70% confluence, they were washed with PBS and cultured in serum-free McCoy's 5A medium. After 48 h, the culture medium was collected. The exosomes were isolated using a gel-filtration chromatography column (qEVSingle, Izon Science, New Zealand). They were then concentrated in an Amicon Ultra-5 (10 kDa nominal molecular weight, Merck Millipore) centrifugal filter to a final volume of 100 µL. The exosome particle size distribution was analyzed using the Izon qNano system (Izon Science, New Zealand). The exosome sample solution was then dried in a centrifugal concentrator (miVac Duo Concentrator; Genevac, Stone Ridge, NY, USA), followed by lysis and exosome protein extraction using RIPA buffer. The lysed sample solution was centrifuged at 12,000 rpm for 20 min at 4 °C, and the supernatant was collected. Five volumes of ice-cold acetone were added to one volume of the supernatant and incubated at −20 °C for 4 h. Next, the precipitated proteins were centrifuged at 12,000 rpm for 15 min at 4 °C. The supernatant was discarded, and the protein pellet was collected for a protein concentration assay and solution digestion.

In-solution digestion

The protein pellet was dissolved in 50 mM ammonium bicarbonate containing 8 M urea and 2 M thiourea. The protein concentration was determined by the Bradford assay (Bio-Rad) and measured using a microplate spectrophotometer reader (Multiskan GO Microplate spectrophotometer, Thermo Scientific, Vantaa, Finland). The proteins were reduced with 10 mM DTT and then alkylated with 55 mM IAA, followed by the addition of 50 mM DTT to quench the remaining IAA. The above-mentioned reduction, alkylation, and quenching steps were incubated at room temperature for 1 h in the dark. Trypsin was used to digest the proteins at an enzyme-to-substrate ratio of 1:40 (*w*/w) for 16 h at 37 °C. The peptide sample solution was dried in a centrifugal concentrator (miVac Duo Concentrator; Genevac, Stone Ridge, NY, USA).

Peptide fractionation by high-pH RP-well plate

Before sample loading, the RP-well plate was washed with 70% ACN. Protein-digested peptides (2 µg) dissolved in 60 µL of deionized H_2O were loaded into the RP-well plate and dried by incubating in an oven at 50 °C. The RP-well plate was then washed with 100 µL of 10 mM NH_4HCO_2 (pH 10, as the flow-through fraction) and sequentially fractionated with 100 µL of seven different elution buffers (5%, 10%, 15%, 20%, 30%, 40%, and 80% ACN in 10 mM NH_4HCO_2, pH 10). All the fractions were subsequently evaporated by centrifugation under vacuum. For nano-LC-MS/MS analysis, the eight fractions were resuspended in 6 µL of 0.1% FA for nano-LC-MS/MS analysis.

High-pH fractionation of a reversed-phase cartridge

The high-pH fractionation by a reverse cartridge was carried out on an Oasis HLB 1 mL Vac Cartridge (30 mg sorbent, 30 µm particle size, Waters Corporation, Milford, MA). All buffers used in HLB separation contained 10 mM NH_4HCO_2

and were adjusted to pH 10 with NH_4OH. After washing with 1 mL of ACN and equilibrating with 1 mL NH_4HCO_2, SKOV3 protein-digested peptides (1 µg) were added with 0.5 mL of NH_4HCO_2 and loaded onto the equilibrated HLB column. Serial elution was carried out stepwise with 0.5 mL of each elution buffer in the order of 10%, 20%, 30%, and 80% ACN/NH_4HCO_2. The fractionated peptide fractions were dried under speed vacuum. The fractions were resuspended in 6 µL of 0.1% FA and subjected to nano-LC-MS/MS analysis.

Nano-LC-MS/MS analysis and database search of HepG2 proteome

HepG2 proteome identification was performed using a captive spray ion source and a hybrid Q-TOF mass spectrometer (maXis Impact, Bruker) coupled with a nanoflow ultra-performance liquid chromatography (UPLC) system (UltiMate 3000 RSLCnano system, Dionex, Amsterdam, Netherlands). Each sample was injected into a commercial trap column (Acclaim PepMap C18, 5 µm 100 Å, 100 µm × 20 mm, Thermo Scientific, USA) at a flow rate of 10 µL min^{-1} for 4 min. The trapped analytes were separated using a commercial analytical column (Acclaim PepMap C18, 2 µm 100 Å, 75 µm × 250 mm, Thermo Scientific, USA) at a flow rate of 300 nL min^{-1}. An ACN/H_2O gradient of 10–40% was used for peptide separation over 60 min. For MS and MS/MS detection, peptides with a charge of 2+, 3+, or 4+ and intensity above 500 counts were chosen for data-dependent acquisition, set to one full MS scan at 1 Hz, and switched to 12 product ion scans with 10 Hz within a mass range of *m*/*z* 50–2000.

The nano-LC-MS/MS spectra were deisotoped, centroided, and converted to .mgf files using DataAnalysis software (version 4.4, Bruker Daltonics), then searched against the UniProt database (downloaded on 5 January 2021) using PEAKS Studio proteomics software version X with the peptide and MS/MS mass tolerance search parameters set at 50 ppm and 0.05 Da, respectively. The search parameters included taxonomy (human), enzyme (trypsin), fixed modification (carbamidomethylation of cysteines), variable modification oxidation (Met), and deamidation (Asn, Gln). The false discovery rate (FDR) was set to 1% for peptide and protein identification.

MicroLC-MS/MS analysis and database search of SKOV3 exosome

The exosome proteome of SKOV3 was identified by microLC-MS/MS using a Dionex UltiMate 3000 RSLC-nano system coupled with an Orbitrap Exploris 480 mass spectrometer (Thermo Fisher Scientific). Each sample was analyzed using a 15 cm RP column (Thermo Scientific EASY-Spray columns, PepMap® RSLC, C18, 150 µm id) with a particle size of 3 µm, 100 Å at a flow rate of 1.2 µL min^{-1} without using a trap column. An ACN/H_2O gradient of 10–45% was used for peptide separation over 90 min. The mass spectra were acquired in a data-dependent manner, with automatic switching between the MS and MS/MS scans using the top-20 method and one micro scan. The MS and MS/MS spectra were acquired at resolutions of 120,000 and 30,000, respectively. The scan range was limited to *m*/*z* 300–1800. The precursor isolation window was *m*/*z* 1.2.

The MS/MS data were processed using Proteome Discoverer software (version 2.4, Thermo Fisher Scientific, USA) for a database search against the human Uniprot FASTA database (42,252 entries, downloaded on 5 May 2019) with the precursor and fragment ion mass tolerance search parameters set at 10 ppm and 0.02 Da, respectively. The search parameters were set to enzyme-trypsin, maximum missed cleavages for trypsin digestion as 2, fixed modification (carbamidomethylation of cysteines), variable modification oxidation (Met), and deamidation (Asn, Gln). The FDR was set to 1% for peptide and protein identification.

Results and discussion

Optimization of sample-loading methods of the RP-well plate

To fabricate the C18-coated RP-well plate, a transparent PDMS film was first coated on the bottom of the ~6.4 mm-diameter sample well of a 96-well plate (Fig. 2a). After loading the C18 particles, followed by incubation and washing, a semi-transparent C18 film was formed at the bottom of the sample well (Fig. 2b).

Owing to the hydrophobic characteristics of the C18 RP-well plate, the loading of hydrophilic sample droplets on the C18-coated surface is a critical step for high-pH RP fractionation. To evaluate the sample-loading efficiency of the RP-well plate, two different sample-loading methods, loading with and without drying, were tested with 2 µg of digested bovine serum albumin (BSA) peptides. The RP-well plate was first washed with 70% ACN to condition the C18 surface. The sample solution (60 µL of deionized water) was loaded immediately and sonicated for 10 s to remove any air bubbles trapped inside the pores of the C18 particles.

In the loading-without-drying method, after sample loading, the RP-well plate was vibrated on a vortex mixer for 15 min at room temperature, and the supernatant was discarded. In the loading-dry method, after sample loading, the RP-well plate was dried in a 50 °C oven for 2 h, and 100 µL of 10 mM NH_4HCO_2 (pH 10) was added to wash the RP-well plate. In both sample-loading methods,

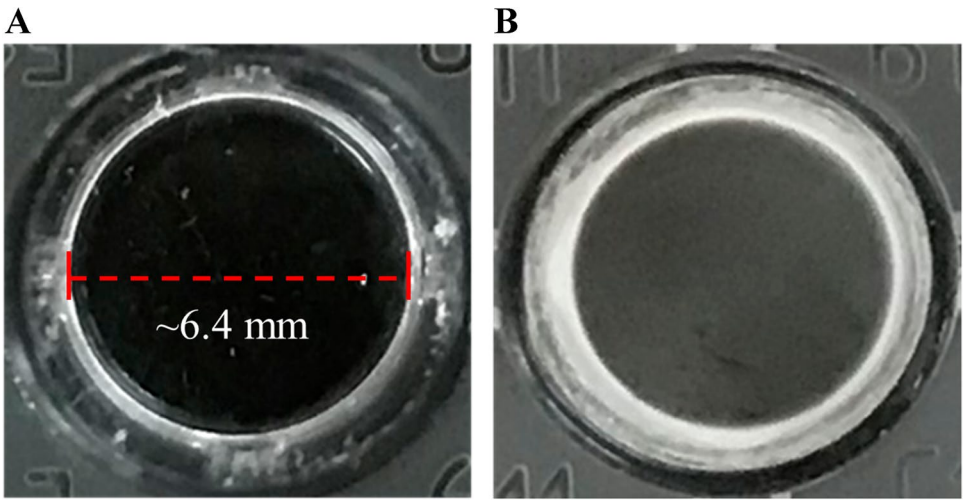

Fig. 2 (**a**) One PDMS-coated sample well (~6.4 mm i.d.) and (**b**) one C18-PDMS-coated sample well of a 96-sample well plate. The image was obtained using an optical camera (NEX-5, Sony, Japan)

the peptides were eluted with 100 µL of 80% ACN containing 10 mM NH_4HCO_2 (pH 10), followed by drying using a speed vacuum and MALDI-TOF analysis. The BSA peptides eluted from the different loading methods were mixed with an internal standard consisting of an ACTH peptide (ACTH fragment, RPVKVYPNGAEDESAEAFPLEF, theoretical $m/z = 2465.1983$) for MALDI-TOF analysis. Two peaks of the trypsin-digested BSA peptides, m/z 1479.8 (LGEYGFQNAILVR, theoretical $m/z = 1479.7954$) and m/z 1567.7 (DAFLGSFLYEYSR, theoretical $m/z = 1567.7427$), were used to compare sample-loading efficiency. Figure 3a shows two representative MALDI spectra acquired using the two different loading methods. In the loading-without-drying method, the peak intensity ratios of m/z 1479.8/2465.2 and m/z 1567.7/2465.2 were ~ 0.12 (standard deviation [SD], 0.013) and 0.06 (SD, 0.004), respectively (Fig. 3b). In the loading-dry method, the peak intensity ratios separately increased to ~0.66 (SD, 0.14) and 0.17 (SD, 0.015), indicating a significant 5.5- and 2.8-fold enhancement in the sample-loading efficiency compared to that with the loading-without-drying method. These results indicate that the peptide binds to the RP-well plate more efficiently during the sample drying process. Therefore, the loading-dry method was used as the sample-loading procedure for subsequent experiments.

Sample capacity

The sample capacity of the RP-well plates was evaluated using BSA digests. Increasing amounts of BSA digests, ranging from 1 to 12 µg, were loaded onto the RP-well plate, and the eluted peptides from each sample were mixed with the same amount of ACTH peptide (m/z 2465.2) that acted as the internal standard. One major peak of the BSA-digested

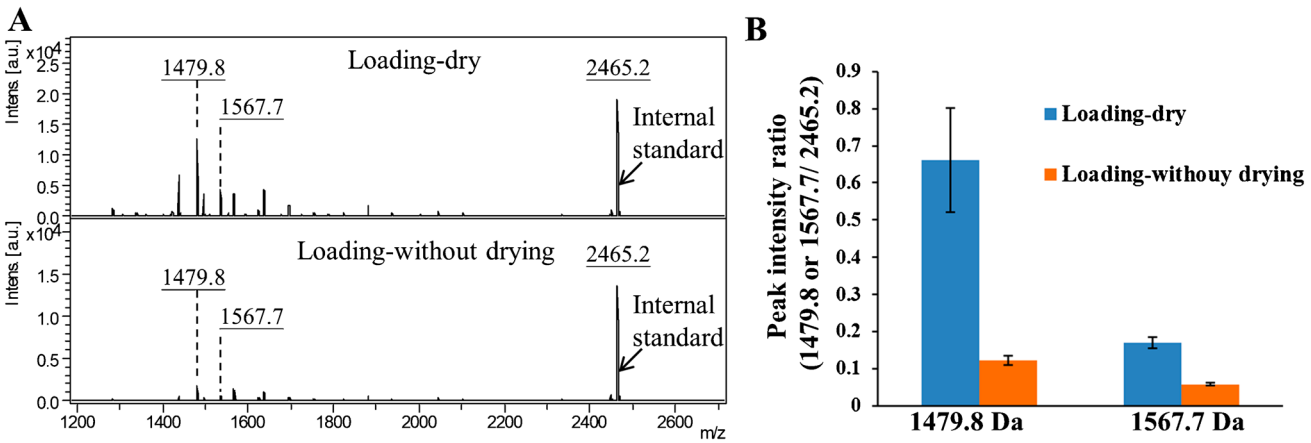

Fig. 3 A comparison of sample loading methods, loading-dry and loading-without-drying, using BSA digests and an ACTH peptide (theoretical m/z: 2465.1983, as an internal standard). (**a**) The representative MALDI-TOF spectrum of loading-dry (upper panel) and loading-without-drying (lower panel) methods. (**b**) The peak ratios of m/z 1479.8/2465.2 and m/z 1567.7/2465.2 in loading-dry and loading-without-drying methods were obtained from three replicated analyses

peptides, *m*/*z* 1479.8, was used to represent the BSA peptide abundance. In the sample capacity design, 5 pmol of ACTH peptide was mixed with the eluted peptides from 1 µg of loaded BSA digests. Therefore, 10, 20, 30, 40, 50, and 60 pmol of ACTH peptide were mixed with the eluted peptides from loading amounts of 2, 4, 6, 8, 10, and 12 µg of the BSA digest prior to MALDI-TOF analysis. The peak ratio (*m*/*z* 1479.8/2465.2) of each sample amount was determined with three triplicate sample well measurements of the three samples. Figure 4 shows a similar peak signal ratio (*m*/*z* 1479.8/2465.2) of ~0.37 from sample loadings between 1 µg and 6 µg, indicating that the protein amount was below the bead capacity. A slightly decreased ratio (~0.19) is observed at 8 and 10 µg, and the ratio drops significantly at 12 µg sample application. Therefore, the maximum sample capacity of the RP-well plate (~6.4 mm) was approximately 6 µg of BSA peptides, and this capacity was sufficient for most of our proteomics studies.

Complex protein digest fractionation by high-pH RP-well plate

To evaluate the fractionation performance of the high-pH RP-well plate, 2 µg of the complex protein digest from the HepG2 cell line was loaded and fractionated with 0% (wash step, flow-through), 5%, 10%, 15%, 20%, 30%, 40%, and 80% ACN in 10 mM NH_4HCO_2 (pH 10), followed by nano-LC-MS/MS analysis. An analytical flowchart of the RP-well plate for high-pH fractionation is shown in Fig. 1.

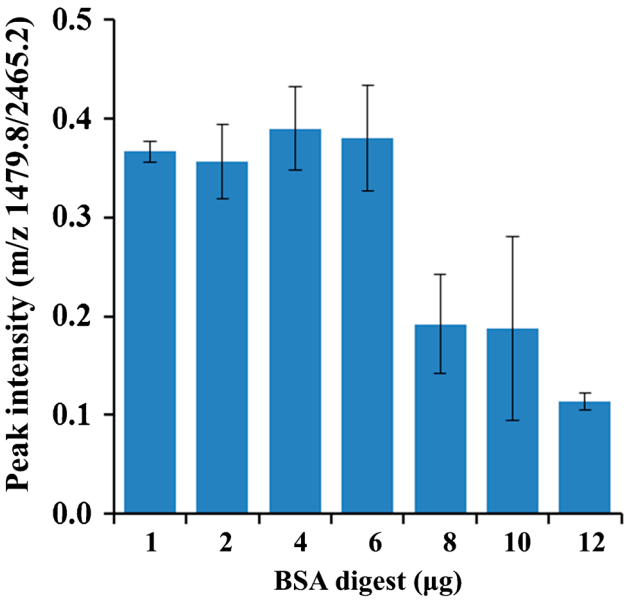

Fig. 4 Sample capacity evaluation of the RP-well plate by MALDI-TOF. The 1, 2, 4, 6, 8, 10, and 12 µg of BSA digests were separately loaded onto the C18 well plate, and eluent was separately mixed with 5, 10, 20, 30, 40, 50, and 60 pmol of ACTH peptide (as an internal standard, *m*/*z* 2465.2) and then subjected to MALDI-TOF analysis. *Y*-axis: the peak ratio of the BSA peak (*m*/*z* 1479.8) to its corresponding ACTH peak signal (*m*/*z* 2465.2). *X*-axis: the loading amount of BSA digests. Each concentration was performed with three spectra

The results showed that the numbers of protein groups/peptides identified in the 0%, 5%, 10%, 15%, 20%, 30%, 40%, and 80% ACN fractions were 690/1576, 795/2039, 819/1967, 835/1877, 803/1931, 709/2292, 557/1550, and 432/993, respectively. (Table 1) Combining the above-identified results, a total of 1324 protein groups and 6186 unique peptides were identified in the eight fractions. However, without fractionation (merging 4 replicate results of a single run), only 715 protein groups and 3625 unique peptides were identified (Fig. 5a). The high-pH RP-well plate fractionation platform was found to provide 1.85- and 1.71-fold increases in the number of identified protein groups and unique peptides, respectively, when compared to the results obtained without fractionation. The results of Venn diagram analysis showed that the overlapped protein groups (percentage distribution) and peptides (percentage distribution) between the one with high-pH RP-well plate fractionation and the one without fractionation were 639 (45.6%) and 2045 (26.3%), respectively (Fig. 5b), indicating that high-pH RP-well plate fractionation provides some complementarity compared to four replicated analyses without fractionation. A grand average of the hydropathy value (GRAVY) calculator (http://www.gravy-calculator.de/) was used to determine the peptide hydrophobicity. A more negative GRAVY score indicates a peptide with more hydrophilic properties, while a more positive GRAVY score indicates a peptide with more hydrophobic properties. A high percentage of hydrophilic peptides were eluted using an elution solvent with a high

Table 1 Numbers of identified protein groups, peptides, and PSMs by nano-LC-MS/MS with and without high-pH RP-well plate fractionation

Samples	Protein groups	Peptides	PSMs*
0% ACN	690	1576	3295
5% ACN	795	2039	4312
10% ACN	819	1967	4351
15% ACN	835	1877	3970
20% ACN	803	1931	3974
30% ACN	709	2292	4767
40% ACN	557	1550	2925
80% ACN	432	993	1794
8 fractions merged	**1324**	**6186**	**29,394**
Single run-1	653	2798	4865
Single run-2	654	2789	4884
Single run-3	633	2772	4878
Single run-3	641	2722	4771
4 of single run merged	**716**	**3626**	**19,385**

**PSMs* peptide spectrum matches

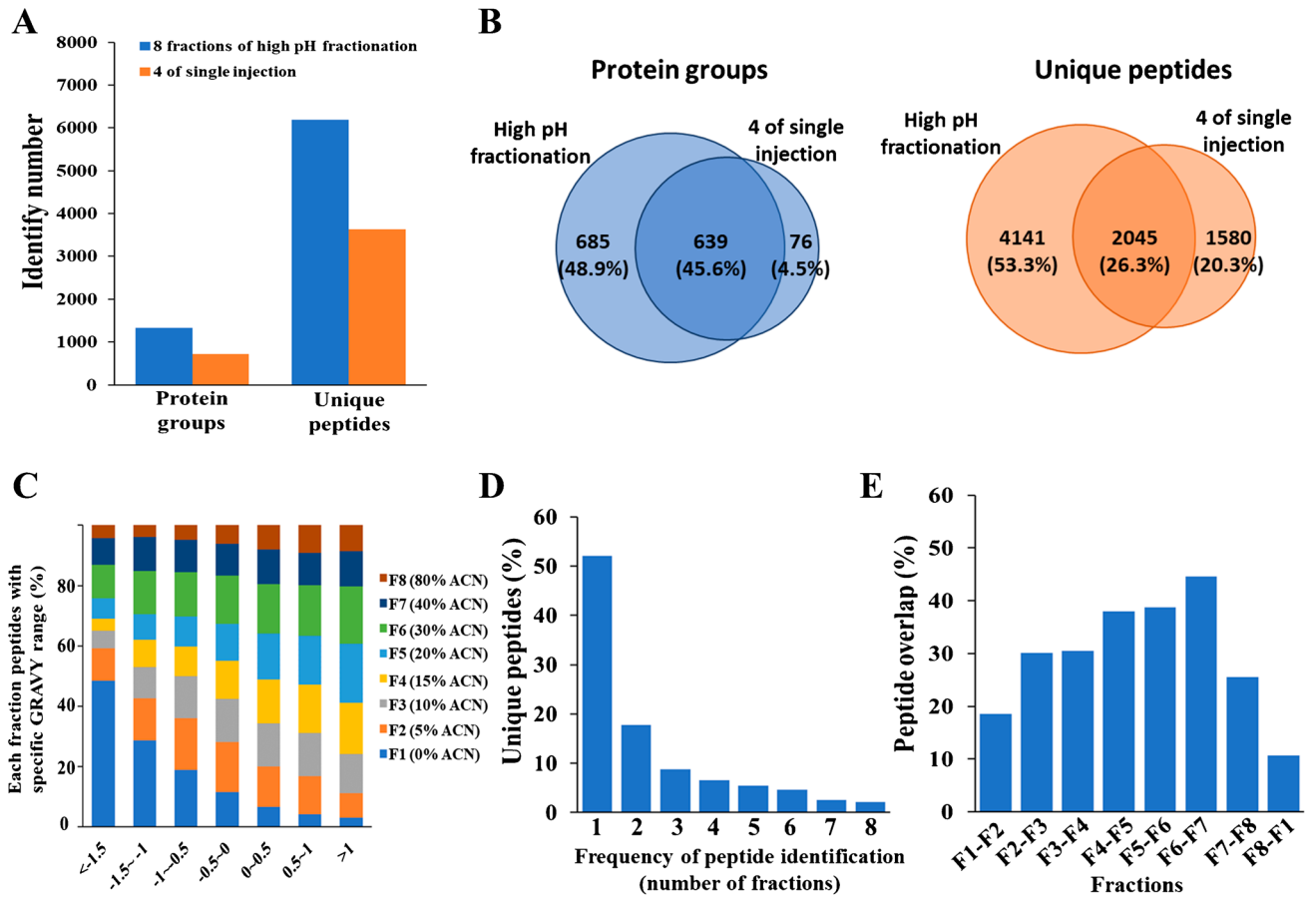

Fig. 5 Evaluation of separation efficiency with high-pH RP-well plate fractionation. (**a**) Identification number of protein groups and unique peptides. (**b**) Venn diagram analysis of overlap number (percentage distribution) of identified protein groups and unique peptides with high-pH RP-well plate fractionation (8 fractions) and without fractionation (merged 4 replicate results of single injection). (**c**) Distribution of GRAVY scores among each fraction. (**d**) The separation efficiency of high-pH RP-well plate fractionation shown as the percentage of peptides found in one or more fractions. (**e**) The overlap between each adjacent fraction is expressed as a percentage of the total peptides identified between the pair of fractions

percentage of H_2O. An increased percentage of hydrophobic peptides were eluted using elution solvents with an increased percentage of ACN (Fig. 5c) Therefore, the high-pH RP-well plate can effectively fractionate peptides according to their hydrophobicity and reduce the sample complexity to improve the sensitivity and specificity of protein identification. The orthogonality of the high-pH RP-well plate fractionation was evaluated with the overlaps of identified unique peptides by each fraction. Figure 5d shows that more than 50% of unique peptides were identified in only one fraction. The overlapping peptide rate between any two adjacent fractions was lower than 50% in all cases (Fig. 5e). The distinct physicochemical characteristics of peptides from the fractionation of the high-pH RP-well plate can significantly improve peptide and protein identification.

The performance of the high-pH RP-well plate was also compared with the performance of an HLB cartridge by using 1 µg of complex protein digests from the SKOV3 cell line with different elution buffers (10%, 20%, 30%, and 80% ACN in 10 mM NH_4HCO_2, pH 10). The identified protein groups/peptides using the RP-well plate and an HLB cartridge were 612/4025 and 598/3064, respectively (Fig. S1), indicating that the RP-well plate provides higher performance in high-pH fractionation than an HLB cartridge does.

Exosome proteome profiling by high-pH RP-well plate and microLC-MS/MS

Exosomes are small (30–150 nm) extracellular vesicles (EVs) secreted from most cell types. They carry specific protein signatures and transmit important signal molecules in cancer progression, angiogenesis, metastatic niche formation, organ-specific metastasis, and tumor microenvironment remodeling [18, 19]. Therefore, exosomes have become a potential resource for elucidating disease mechanisms, drug delivery, and disease biomarker discovery. Various exosome

isolation methods have been developed, including ultracentrifugation, magnetic beads, and SEC, as well as density-based and filtration-based isolation methods. To examine the quality of the isolated exosomes, their size distribution, morphology, quantity, and biochemical composition were measured [20]. Some protein markers, such as TSG101, HSP90AB1 (HSP84), ALIX, CD59, CD81, and calnexin, are usually used for exosome characterization [21, 22], and western blotting has traditionally been the analytical method of choice. However, the western blotting assay usually requires several micrograms of protein for one protein identification [23, 24]. Exosomes are valuable samples typically available only in trace amounts [25, 26]; nano/microLC-MS/MS has gradually become a more attractive approach for exosome characterization and disease biomarker discovery. Several studies have reported the proteomic signatures of exosomes derived from biological fluids such as plasma, urine, cerebrospinal fluid (CSF), and cell culture medium [27–29]. Zhang et al. identified 262 proteins from the LC-MS/MS analysis of exosomes extracted from the plasma of ovarian cancer patients [28]. Diederick et al. identified 732 proteins derived from SKOV3 ovarian cancer cells through proteomic analysis [29]. In our exosome proteome study, exosomes were obtained from SKOV3 cells (three 10-cm dishes) by incubation with serum-free medium for 48 h, followed by the collection of the medium (24 mL) for exosome isolation and protein purification. Izon qNano system analysis revealed that the diameter of most particles was in the range of 90–150 nm (Fig. 6a). After protein purification, only a small amount of protein (9.2 µg) was harvested from 24 mL of the medium. Herein, the proteomic profiling of ~2 µg of protein digest of SKOV3 cell-released exosomes was performed with high-pH well plate fractionation, and ~ 1 µg of the fractionated sample amount was analyzed. To increase the sensitivity, a microLC system coupled to an Orbitrap Exploris 480 mass spectrometer was used to detect exosome proteins. A total of 2294 protein groups and 14,023 unique peptides were identified (Fig. 6b and Table S1).

According to a published study [21], a total of 104 reported exosome markers were identified in this study (Table S2). These include transmembrane anchored proteins (CD9, CD59, and integrin family), membrane-binding proteins for transport (Alix, TSG101, and Flot 1), and heat-shock proteins (Hsp60, Hsp70, and Hsp90). However, without high-pH well plate fractionation, the merged triplicate results of a single run showed that the number of protein groups and identified peptides decreased to 540 and 3939, respectively (Fig. 6b). Furthermore, only 42 exosome markers were detected, representing a significantly lower protein coverage and fewer identified peptides compared to the results from high-pH fractionation (Table S2). Compared with the western blotting assay, which usually uses several to dozens of micrograms for one protein identification [23, 24], the use of ~1 µg of the fractionated sample for microLC-MS/MS analysis renders this a sensitive platform for deep exosome proteome and exosome characterization.

Conclusion

In this study, we fabricated a C18-functionalized RP-well plate and evaluated its performance in the proteomic analysis of HepG2 cells and SKOV3 exosomes. The RP-well plate can efficiently increase the number of identified peptides and proteins for deeper proteome analysis. This approach has the advantages of being a simple fabrication procedure with high throughput, microscale fractionation, and easy manual operation. Therefore, this platform could be promising for the deep proteome analyses of exosomes, needle biopsies, isolated cell organelles, and other samples with limited and valuable protein amounts.

Supplementary Information The online version contains supplementary material available at https://doi.org/10.1007/s00216-022-03892-0.

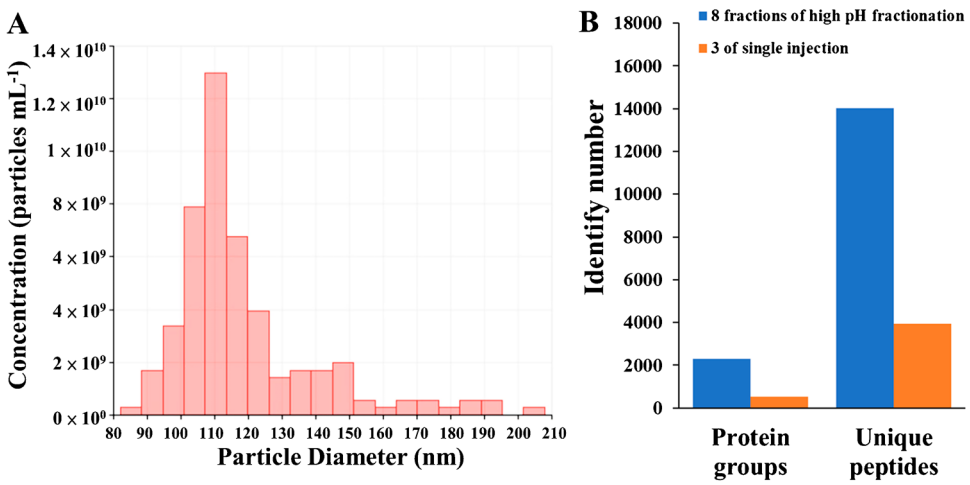

Fig. 6 Identification of exosome. (**a**) Size distribution of exosomes isolated from SKOV3 cells. (**b**) The number of identified unique peptides and proteins of exosomes with and without high-pH RP-well plate fractionation

Author contributions **Yu-Ching Liu:** conceptualization, methodology, software, validation, investigation, data curation, writing—original draft. **Yu-Ting Huang:** methodology, validation, data curation. **Chao-Jung Chen:** conceptualization, methodology, visualization, investigation, supervision, writing modification, writing—review & editing, project administration, funding acquisition.

Funding This work was supported by grants from the Taiwan Ministry of Science and Technology (MOST109–2113-M-039-001), China Medical University (CMU109-MF-04), and China Medical University Hospital (DMR-109-148, DMR-110-034).

Data availability The mass spectrometry proteomics data have been deposited in the MassIVE Consortium with the dataset identifier MSV 000087860 (https://doi.org/10.25345/C5WR7T).

Declarations

Declaration of competing interest The authors declare no competing interests.

References

1. Solovyeva EM, Lobas AA, Kopylov AT, Ilina IY, Levitsky LI, Moshkovskii SA, et al. FractionOptimizer: a method for optimal peptide fractionation in bottom-up proteomics. Anal Bioanal Chem. 2018;410(16):3827–33.
2. Rappsilber J, Mann M, Ishihama Y. Protocol for micro-purification, enrichment, pre-fractionation and storage of peptides for proteomics using StageTips. Nat Protoc. 2007;2(8):1896–906.
3. Zhu MZ, Li N, Wang YT, Liu N, Guo MQ, Sun BQ, et al. Acid/salt/pH gradient improved resolution and sensitivity in proteomics study using 2D SCX-RP LC-MS. J Proteome Res. 2017;16(9):3470–5.
4. Kitata RB, Dimayacyac-Esleta BR, Choong WK, Tsai CF, Lin TD, Tsou CC, et al. Mining missing membrane proteins by high-pH reverse-phase StageTip fractionation and multiple reaction monitoring mass spectrometry. J Proteome Res. 2015;14(9):3658–69.
5. Horth P, Miller CA, Preckel T, Wenz C. Efficient fractionation and improved protein identification by peptide OFFGEL electrophoresis. Mol Cell Proteomics. 2006;5(10):1968–74.
6. Magdeldin S, Elguoshy A, Yoshida Y, Hirao Y, Xu B, Zhang Y, et al. Complementary protein and peptide OFFGEL fractionation for high-throughput proteomic analysis. Anal Chem. 2015;87(16):8481–8.
7. Ow SY, Salim M, Noirel J, Evans C, Wright PC. Minimising iTRAQ ratio compression through understanding LC-MS elution dependence and high-resolution HILIC fractionation. Proteomics. 2011;11(11):2341–6.
8. Hu L, Boos KS, Ye M, Wu R, Zou H. Selective on-line serum peptide extraction and multidimensional separation by coupling a restricted-access material-based capillary trap column with nanoliquid chromatography-tandem mass spectrometry. J Chromatogr A. 2009;1216(28):5377–84.
9. Gilar M, Olivova P, Daly AE, Gebler JC. Two-dimensional separation of peptides using RP-RP-HPLC system with different pH in first and second separation dimensions. J Sep Sci. 2005;28(14):1694–703.
10. Wang Y, Yang F, Gritsenko MA, Wang Y, Clauss T, Liu T, et al. Reversed-phase chromatography with multiple fraction concatenation strategy for proteome profiling of human MCF10A cells. Proteomics. 2011;11(10):2019–26.
11. Gilar M, Jaworski A, Olivova P, Gebler JC. Peptide retention prediction applied to proteomic data analysis. Rapid Commun Mass Spectrom. 2007;21(17):2813–21.
12. Stein DR, Hu X, McCorrister SJ, Westmacott GR, Plummer FA, Ball TB, et al. High pH reversed-phase chromatography as a superior fractionation scheme compared to off-gel isoelectric focusing for complex proteome analysis. Proteomics. 2013;13(20):2956–66.
13. Yue XS, Hummon AB. Combination of multistep IMAC enrichment with high-pH reverse phase separation for in-depth phosphoproteomic profiling. J Proteome Res. 2013;12(9):4176–86.
14. Han D, Jin J, Woo J, Min H, Kim Y. Proteomic analysis of mouse astrocytes and their secretome by a combination of FASP and StageTip-based, high pH, reversed-phase fractionation. Proteomics. 2014;14(13–14):1604–9.
15. Dimayacyac-Esleta BR, Tsai CF, Kitata RB, Lin PY, Choong WK, Lin TD, et al. Rapid high-pH reverse phase StageTip for sensitive small-scale membrane proteomic profiling. Anal Chem. 2015;87(24):12016–23.
16. Naldrett MJ, Zeidler R, Wilson KE, Kocourek A. Concentration and desalting of peptide and protein samples with a newly developed C18 membrane in a microspin column format. J Biomol Tech. 2005;16(4):423–8.
17. Liao HY, Tsai FJ, Lai CC, Tseng MC, Hsu CY, Chen CJ. Rapid fabrication of functionalized plates for peptides, glycopeptides and protein purification and mass spectrometry analysis. Analyst. 2016;141(7):2183–90.
18. Costa-Silva B, Aiello NM, Ocean AJ, Singh S, Zhang H, Thakur BK, et al. Pancreatic cancer exosomes initiate pre-metastatic niche formation in the liver. Nat Cell Biol. 2015;17(6):816–26.
19. Hoshino A, Costa-Silva B, Shen TL, Rodrigues G, Hashimoto A, Tesic Mark M, et al. Tumour exosome integrins determine organotropic metastasis. Nature. 2015;527(7578):329–35.
20. Khatun Z, Bhat A, Sharma S, Sharma A. Elucidating diversity of exosomes: biophysical and molecular characterization methods. Nanomedicine (Lond). 2016;11(17):2359–77.
21. Thery C, Witwer KW, Aikawa E, Alcaraz MJ, Anderson JD, Andriantsitohaina R, et al. Minimal information for studies of extracellular vesicles 2018 (MISEV2018): a position statement of the International Society for Extracellular Vesicles and update of the MISEV2014 guidelines. J Extracell Vesicles. 2018;7(1):1535750.
22. Gandham S, Su X, Wood J, Nocera AL, Alli SC, Milane L, et al. Technologies and standardization in research on extracellular vesicles. Trends Biotechnol. 2020;38(10):1066–98.
23. Welinder C, Ekblad L. Coomassie staining as loading control in Western blot analysis. J Proteome Res. 2011;10(3):1416–9.
24. Taylor SC, Berkelman T, Yadav G, Hammond M. A defined methodology for reliable quantification of Western blot data. Mol Biotechnol. 2013;55(3):217–26.
25. Patel GK, Khan MA, Zubair H, Srivastava SK, Khushman M, Singh S, et al. Comparative analysis of exosome isolation methods using culture supernatant for optimum yield, purity and downstream applications. Sci Rep. 2019;9(1):5335.
26. Hou R, Li Y, Sui Z, Yuan H, Yang K, Liang Z, et al. Advances in exosome isolation methods and their applications in proteomic analysis of biological samples. Anal Bioanal Chem. 2019;411(21):5351–61.
27. Jablonska J, Pietrowska M, Ludwig S, Lang S, Thakur BK. Challenges in the isolation and proteomic analysis of cancer exosomes-implications for translational research. Proteomes. 2019;7(2):22.
28. Zhang W, Ou X, Wu X. Proteomics profiling of plasma exosomes in epithelial ovarian cancer: a potential role in the

coagulation cascade, diagnosis and prognosis. Int J Oncol. 2019;54(5):1719–33.
29. Cheng L, Zhang K, Qing Y, Li D, Cui M, Jin P, et al. Proteomic and lipidomic analysis of exosomes derived from ovarian cancer cells and ovarian surface epithelial cells. J Ovarian Res. 2020;13(1):9.

Publisher's note Springer Nature remains neutral with regard to jurisdictional claims in published maps and institutional affiliations.